

Flexible Sensory Representations in Auditory Cortex Driven by Behavioral Relevance

Highlights

- Passive sound experience causes habituation of sensory representations in A1
- Habituation involves an increase in inhibition of layer 2/3 pyramidal cells
- Habituation reflects the selective upregulation of SOM interneuron activity
- Sound-guided behavior decreases SOM cell activity and rapidly reverses habituation

Authors

Hiroyuki K. Kato, Shea N. Gillet,
Jeffrey S. Isaacson

Correspondence

h1kato@ucsd.edu

In Brief

Kato et al. demonstrate that daily sound experience upregulates SOM interneuron activity in A1 and causes “habituation” of sound representations. Sound-guided behavior reverses these effects, indicating that sensory representations are bidirectionally modified based on the behavioral relevance of sensory stimuli.

Flexible Sensory Representations in Auditory Cortex Driven by Behavioral Relevance

Hiroyuki K. Kato,^{1,*} Shea N. Gillet,¹ and Jeffrey S. Isaacson¹

¹Center for Neural Circuits and Behavior and Department of Neurosciences, University of California, San Diego, La Jolla, CA 92093, USA

*Correspondence: h1kato@ucsd.edu

<http://dx.doi.org/10.1016/j.neuron.2015.10.024>

SUMMARY

Animals require the ability to ignore sensory stimuli that have no consequence yet respond to the same stimuli when they become useful. However, the brain circuits that govern this flexibility in sensory processing are not well understood. Here we show in mouse primary auditory cortex (A1) that daily passive sound exposure causes a long-lasting reduction in representations of the experienced sound by layer 2/3 pyramidal cells. This habituation arises locally in A1 and involves an enhancement in inhibition and selective upregulation in the activity of somatostatin-expressing inhibitory neurons (SOM cells). Furthermore, when mice engage in sound-guided behavior, pyramidal cell excitatory responses to habituated sounds are enhanced, whereas SOM cell responses are diminished. Together, our results demonstrate the bidirectional modulation of A1 sensory representations and suggest that SOM cells gate cortical information flow based on the behavioral relevance of the stimulus.

INTRODUCTION

An important aspect of brain function is the flexibility to generate behavioral output based on the relevance of sensory input. Neural representations of sensory input are also likely to be flexibly regulated based on behavioral demand. Indeed, in primary areas of sensory cortex, stimulus representations can change in response to a variety of behaviorally relevant factors such as locomotion, arousal, and attention (Desimone and Duncan, 1995; Fritz et al., 2003; McGinley et al., 2015; Niell and Stryker, 2010; Schneider et al., 2014; Zhou et al., 2014). The flexibility of neural representations in primary sensory cortex may play an important role in regulating the salience of information processed by higher brain areas and the subsequent generation of appropriate behavioral output.

Behavioral relevance is not a fixed attribute of sensory stimuli; rather it is constantly updated based on the previous experiences of the individual animal. Indeed, sensory experience is a potential trigger for changes in cortical sensory representations. For example, studies in primary auditory cortex (A1) have established early developmental critical periods during which

long-term changes in cortical circuitry are elicited by changes in experience such as sensory deprivation or patterned acoustic stimulation (Barkat et al., 2011; de Villers-Sidani et al., 2007; Zhang et al., 2001). In adults, however, long-term changes in auditory cortex circuits are believed to require associative conditioning. For instance, pairing tones of a particular frequency with foot shocks or stimulation of subcortical neuromodulatory systems shifts the frequency tuning of individual neurons in A1 toward the frequency of the conditioned tone (Bakin and Weinberger, 1996; Bakin et al., 1996; Froemke et al., 2013). Similarly, reward association is also reported to induce changes in auditory sensory representations (Blake et al., 2002; Rutkowski and Weinberger, 2005). In the absence of associative conditioning, passive sensory stimulation alone can induce short-term (milliseconds to seconds) “stimulus-specific adaptation” in auditory cortex (Ulanovsky et al., 2003) and subcortical structures (Anderson et al., 2009; Malmierca et al., 2009). However, difficulty in monitoring the dynamics of sensory representations in the same animal over long timescales has hampered investigation of the long-term effects of passive sensory experience on cortical auditory coding.

Here we take advantage of chronic two-photon calcium imaging to investigate how experience and changes in the behavioral relevance of acoustic stimuli alter sensory representations in adult auditory cortex. We show that brief daily experience with simple tones causes a progressive reduction (“habituation”) in the representation of the experienced tone by layer 2/3 (L2/3) pyramidal cells. Tone-evoked responses of local somatostatin-expressing inhibitory neurons (SOM cells), but not parvalbumin-expressing neurons (PV cells), are enhanced by daily experience, suggesting that long-lasting habituation involves a selective increase in SOM cell-mediated inhibition. Furthermore, we demonstrate that sensory representations of habituated tones are rapidly enhanced when mice engage in sound-guided behavior and that this change is associated with the decrease of SOM cell activity. Thus, sensory representations in A1 can be bidirectionally modulated based on whether or not behavioral relevance is attached to the sensory stimulus.

RESULTS

Chronic Imaging of A1 Sound Representations in Awake Mice

We combined macroscopic imaging of intrinsic signals and two-photon cellular-resolution Ca^{2+} imaging to study sensory representations in A1 of head-fixed mice (Figure 1A; Boyd et al., 2015).

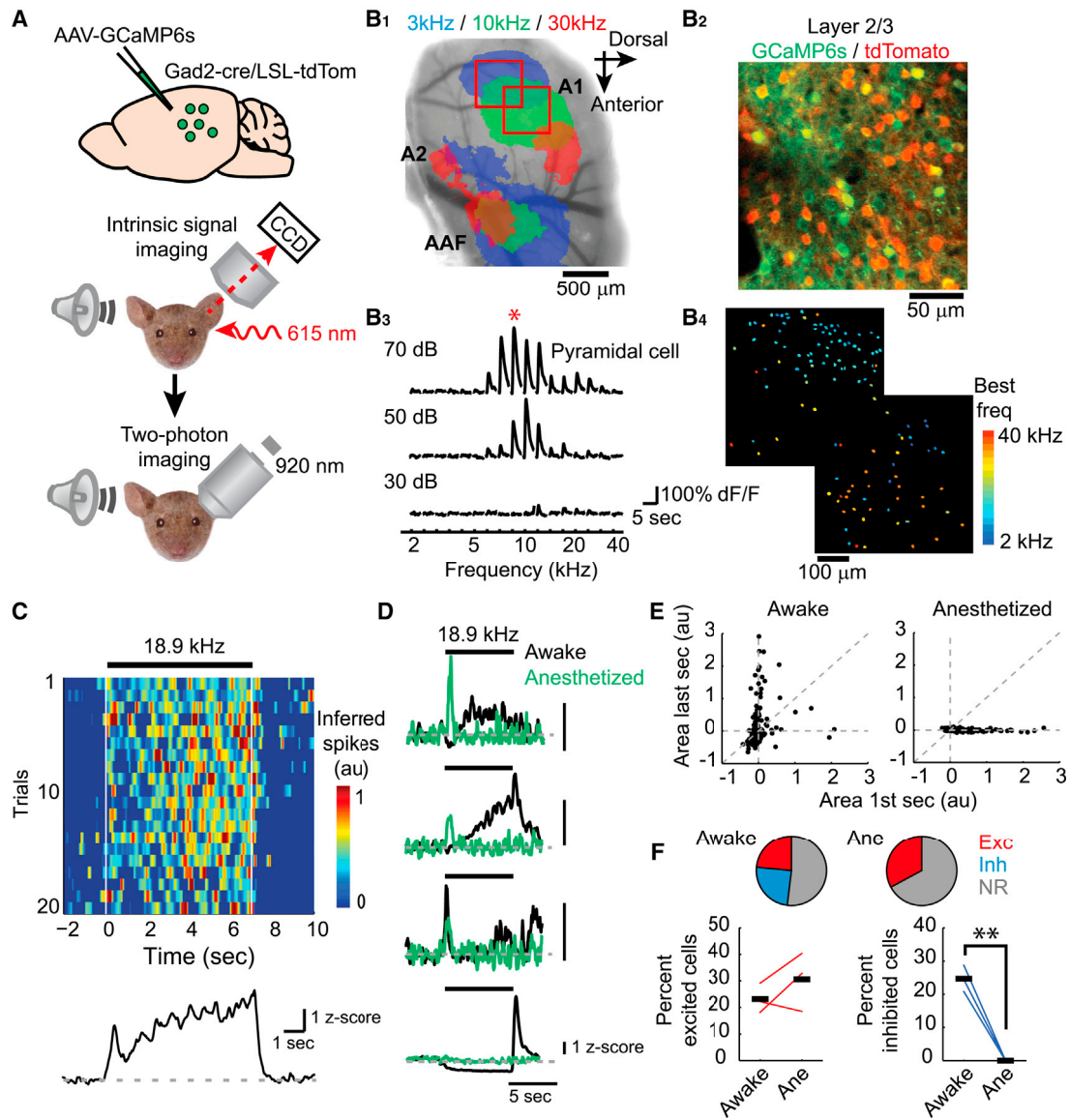


Figure 1. Imaging Sensory Representations in A1 Layer 2/3 Pyramidal Cells

(A) Top: a viral vector expressing GCaMP6s is injected into auditory cortex of mice heterozygous for *Gad2-IRES-Cre* and *ROSA-LSL-tdTomato*. Bottom: initial mapping of auditory cortical areas by intrinsic signal imaging is followed by cellular-level two-photon calcium imaging of A1 in awake mice.

(B₁) Intrinsic signal imaging from one mouse showing responses to pure tones (3, 10, and 30 kHz) superimposed on the auditory cortex surface vasculature. Three auditory cortical areas (A1, A2, and AAF) are identified based on tonotopic patterns. Red squares indicate the locations of subsequent two-photon imaging in (B₄).

(B₂) In vivo two-photon image of GCaMP6s- (green) and tdTomato- (red) expressing cells in L2/3 of A1 of an awake mouse.

(B₃) Responses of a representative L2/3 pyramidal cell to tone pips of 17 different frequencies (columns) at three intensities (rows). An average trace across five trials is shown for each tone, and the red asterisk indicates the best frequency.

(B₄) Activity map showing the best frequency of individual pyramidal cells within fields indicated in (B₁).

(C) Top: heat map of inferred spikes for a representative pyramidal cell in response to a 7-s, 18.9-kHz tone over 20 trials. Bottom: average trace of inferred spikes across trials. au, arbitrary units.

(D) Prolonged tones evoke responses with diverse temporal patterns in awake mice but elicit only transient excitation under anesthesia. Average responses of four pyramidal cells to an 18.9-kHz tone in the awake (black) and anesthetized (green) state.

(E) Pyramidal cell responses are more temporally dynamic in the awake state. Left: comparison of the inferred spike rates during the first 1 s and the last 1 s of the tone in individual cells in the awake state. Each point represents a single cell ($n = 3$ mice, 239 cells). Right: the same cells in the anesthetized state.

(F) Top: fraction of cells with significant excitatory (Exc) and inhibitory (Inh) responses across mice. NR, nonresponding cells. Bottom: fraction of excited and inhibited cells shown separately for individual mice. ** $p < 0.01$.

See also Figure S1.

We used adeno-associated virus (AAV) vectors to express the calcium indicator GCaMP6s (Chen et al., 2013) in auditory cortex neurons of transgenic mice containing the activity-independent reporter tdTomato in GABAergic neurons (*Gad2-IRES-Cre* × *ROSA-LSL-tdTomato*). This allowed us to optically distinguish glutamatergic pyramidal cells (green) from GABAergic interneurons (green + red) (Figure 1B2). Two to three weeks following virus injection and the implantation of a glass window over auditory cortex, we performed intrinsic signal imaging to map the precise position of A1. Responses to pure tones of three frequencies (3, 10, and 30 kHz) routinely revealed three cortical regions that displayed tonotopic organization (Figure 1B1). These results are in agreement with previous coarse mapping studies of mouse auditory cortex (Guo et al., 2012; Issa et al., 2014) that identified the areas as A1, secondary auditory cortex (A2), and the anterior auditory field (AAF). We registered intrinsic signal images to the surface vasculature to guide cellular imaging to fields within A1.

We used brief tone pips (ranging from 2 to 40 kHz and 30 to 70 dB, 1-s duration) and two-photon imaging of GCaMP6s to examine the response properties of individual pyramidal cells in L2/3 (120–250 μm beneath the pial surface). On average, 31.0% ± 4.4% of GCaMP6s-expressing pyramidal cells (n = 1,480 cells, 16 imaging fields, 8 mice) revealed increases in activity (measured as dF/F) in response to at least one frequency. Consistent with previous studies of A1 (Rothschild et al., 2010; Schreiner et al., 2010; Sutter, 2000), 42% of responsive L2/3 pyramidal cells (n = 550) displayed “V-shaped” tonal receptive fields (TRFs; Figure 1B3). To examine the spatial organization of tuning properties at the cellular level, we constructed activity maps representing the best frequencies of responsive cells. As previously reported for cellular calcium imaging in A1 (Bandyopadhyay et al., 2010; Issa et al., 2014; Rothschild et al., 2010), we observed a cellular-level tonotopic organization that coarsely adhered to the tonotopic axis identified by macroscopic imaging (Figure 1B4). Together, these results indicate that we can reliably target cells in A1, and all subsequent experiments were conducted in the middle-frequency (10–20 kHz) region of this cortical area.

Whereas most studies of auditory processing have been performed in anesthetized animals, sensory representations could be different in the awake state. For example, some studies of cortical neurons suggest that tones evoke primarily transient activity at sound onset or offset (DeWeese et al., 2003; Volkov and Galazjuk, 1991), whereas other studies have highlighted the fact that sustained responses are more prevalent in the awake state (Luczak et al., 2013; Wang et al., 2005). We next examined the temporal features of auditory responses under our conditions using prolonged (5–9 s) pure tones. To better estimate the time course of evoked activity, we calculated the inferred spike rate from changes in fluorescence using deconvolution (Vogelstein et al., 2010) and used a single frequency based on the tone that activated the most cells during TRF mapping of each field. In awake mice, prolonged tones evoked reproducible responses in individual pyramidal cells across trials (Figure 1C) and individual cells displayed a variety of temporal patterns: sustained increases in activity, responses that ramped up, transient activity at tone onset, and sustained inhibitory responses (Figures 1C

and 1D). These features are not due to our imaging approach, because we observed similar patterns of excitation and inhibition in electrophysiological recordings of single-unit activity (Figure S1). Measuring the area of the response during the tone revealed that a similar fraction of cells responded with net excitation or inhibition (Figure 1F; excitation: 23.2% ± 3.2%; inhibition: 24.7% ± 2.3%; n = 239 cells, 3 mice). We next imaged the same cell populations during anesthesia to test whether the temporal structure of responses and prominent inhibition was dependent on brain state. Remarkably, tones evoked only transient excitation at sound onset or offset in the anesthetized state (Figures 1D and 1E). To quantify the change in response kinetics, we calculated an onset response index for each excited cell as (onset response – sustained response)/(onset response + sustained response), where onset and sustained responses represent the inferred spike rates during the first and last second of tones, respectively. This index indicated a significant shift toward transient responses during anesthesia (awake: -0.46 ± 0.12 ; anesthetized: 0.83 ± 0.04 ; $p < 0.001$). Furthermore, in contrast to the equal proportion of cells with excitatory and inhibitory responses during wakefulness, inhibitory responses were entirely absent in the anesthetized state (Figure 1F; excitation: 30.6% ± 6.4%; inhibition: 0%). These results demonstrate that sound representations are dramatically different in the anesthetized state and highlight the importance of studying cortical processing during wakefulness.

Daily Passive Sound Experience Produces Long-Lasting Cortical Habituation

Having characterized responses to prolonged pure tones in naive mice, we next investigated how they are affected by repeated experience. To address this, we imaged the activity of ensembles of L2/3 pyramidal cells across 5 days of passive exposure to the same tones (Figure 2A; 70 dB, 5- to 9-s duration, 200 trials/day). Under these conditions, brief daily experience (total of ~20 min/day) caused a marked change in A1 sound representations: cells excited by the tone became sparser. Remarkably, experience also caused a dramatic increase in the number of cells inhibited by the tone (Figure 2A), and cells that were initially excited by the tone in naive mice switched to being inhibited after daily experience (Figure 2B). Overall, the fraction of excited cells in each imaging field (n = 519 cells, 8 mice) was markedly diminished (Figure 2C) (day 1: 19.9% ± 2.7%; day 5: 6.1% ± 1.1%; $p = 0.001$) and the fraction of inhibited cells doubled (day 1: 12.5% ± 3.4%; day 5: 25.4% ± 4.2%; $p = 0.002$). Consequently, the ratio of excited to inhibited cells was reduced by 10-fold (2.96 ± 0.80 on day 1 to 0.32 ± 0.08 on day 5; $p = 0.02$). We studied the time course of the changes in response strength using a separate change index (CI) for excitation and inhibition (Experimental Procedures). Excitation progressively decreased with little recovery from previous days, whereas inhibition gradually increased (Figure 2D). The daily change index calculated between day 1 and day 5 indicated a significant reduction in the strength of excitation (Figure 2E; CI = -0.63 ± 0.05 , $p < 0.001$). Although data analyses using spike inference can be affected by signal-to-noise ratio (Lütcke et al., 2013), our conclusions were identical when dF/F values were used for analyses. These findings were also insensitive to other changes in

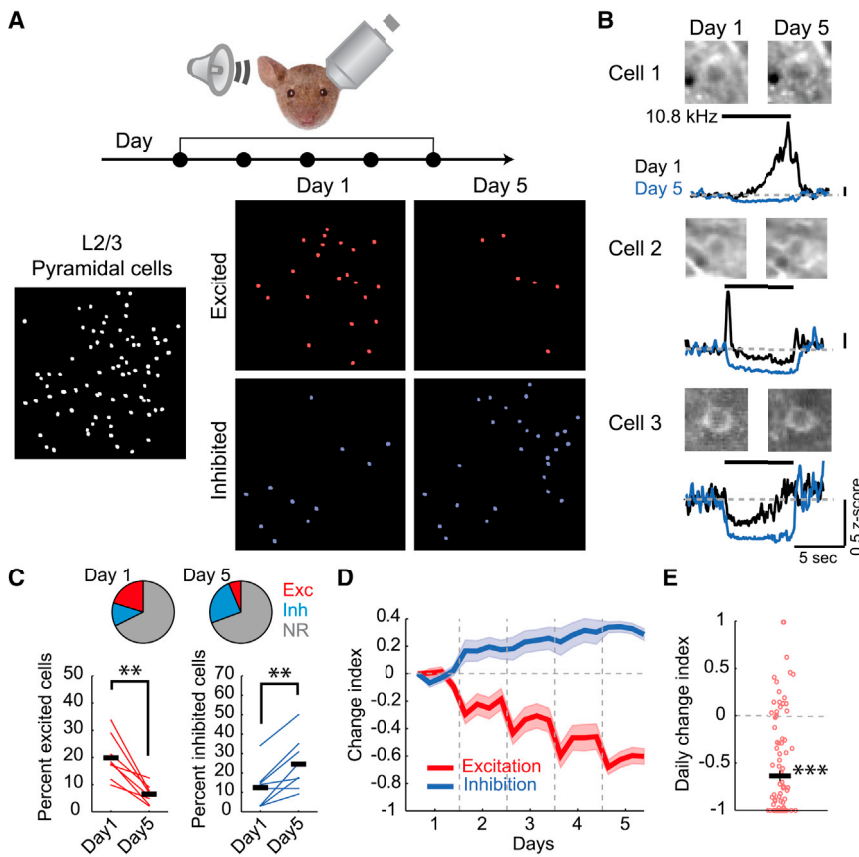


Figure 2. Daily Passive Sound Experience Induces a Long-Lasting Habituation of Sensory Representations

(A) Top: schematic of the protocol for sound experience and chronic imaging. Mice were passively exposed to 5- to 9-s tones for 200 trials/day over 5 consecutive days. Bottom: maps of L2/3 pyramidal cell activity from one animal in response to 18.9-kHz tones show that excitation becomes sparser and inhibition becomes denser after 5 days of sound experience. Bottom left: map of all imaged pyramidal cells.

(B) Average sound-evoked responses from three cells on day 1 (black) and day 5 (blue).

(C) Top: fraction of cells with significant excitatory and inhibitory responses across mice. Bottom: fraction of cells shown separately for individual mice (n = 8 mice, 519 cells).

(D) Average (solid) and SEM (shading) of the change index across days. Each data point represents a block of 50 trials. Excitatory response amplitudes gradually decrease and inhibitory responses increase over days.

(E) Daily change index of excitatory responses in individual cells reveals a reduction in the strength of excitation from day 1 to day 5 (n = 104 excited cells).

Error bar represents SEM. **p < 0.01, ***p < 0.001. See also Figures S1–S5.

image analysis parameters, such as different amounts of neuropil signal subtraction (Figure S2). Indeed, electrophysiological recordings of single-unit activity revealed a similar shift to tone-evoked inhibition after daily sound experience (Figure S1). Furthermore, cell TRFs measured before and after experience indicated that the changes in excitation were selective for the experienced frequency (Figure S3), ruling out the possibility that our results reflect a nonspecific effect due to changes in brain state. Taken together, these findings indicate that repeated passive experience over days induces a progressive habituation in the representation of the experienced tone in A1 L2/3 pyramidal cells. Furthermore, habituation in A1 is not just a simple withdrawal of excitation; rather it also reflects a pronounced increase in inhibitory responses to the experienced stimulus. This sensory habituation provides a way for the cortex to filter out information lacking behavioral relevance.

Increased Inhibition after Habituation Reflects the Upregulation of SOM Cell Activity in A1

We next considered whether the experience-dependent plasticity of auditory responses in L2/3 pyramidal cells arises locally within A1 or whether it is inherited from upstream subcortical structures, such as thalamus or inferior colliculus. To address this question, we selectively targeted GCaMP6s to layer 4 (L4) thalamorecipient neurons using Cre-dependent vectors and *Scnn1a-Cre* mice (Figure 3A). We imaged the responses of L4

cells in these mice across 5 days of experience to prolonged tones (Figure 3B). Like L2/3 pyramidal cells, L4 neurons in naive mice (day 1) responded to prolonged pure tones with diverse temporal patterns (Figure 3C). However, after 5 days of passive tone exposure, there was only a minor reduction in the fraction of cells with excitatory responses to the experienced tone (Figure 3D; day 1: 25.0% ± 2.8%; day 5: 20.1% ± 5.7%; p = 0.42, n = 4 mice, 398 cells). Interestingly, the small change in excited cells was accompanied by a similar reduction in the fraction of inhibited cells (Figure 3D; day 1: 23.3% ± 5.5%; day 5: 17.1% ± 2.2%; p = 0.22). Thus, in contrast to the 10-fold decrease in the ratio of excited to inhibited L2/3 pyramidal cells produced by passive experience, this ratio remained unchanged in L4 (day 1: 1.50 ± 0.46; day 5: 1.35 ± 0.46; p = 0.36). Furthermore, the strength of excitatory responses showed only a small decrease during day 1 that remained virtually constant during the additional days of tone experience (Figure 3E). This reduction in excitation was matched by a similar reduction in the magnitude of inhibitory responses (Figure 3E). Overall, the daily change index between day 1 and day 5 indicated only a minor reduction in the strength of excitation across the cell population (Figure 3F; CI = -0.12 ± 0.07, p = 0.11). These weak effects of experience in L4 thalamorecipient cells make it unlikely that the marked habituation in L2/3 is inherited from upstream subcortical sources, and suggest that experience produces changes in the cortex itself.

Given our results suggesting a cortical origin for the increased inhibition of L2/3 pyramidal cells, we examined whether local GABAergic interneurons contribute to habituation. We first

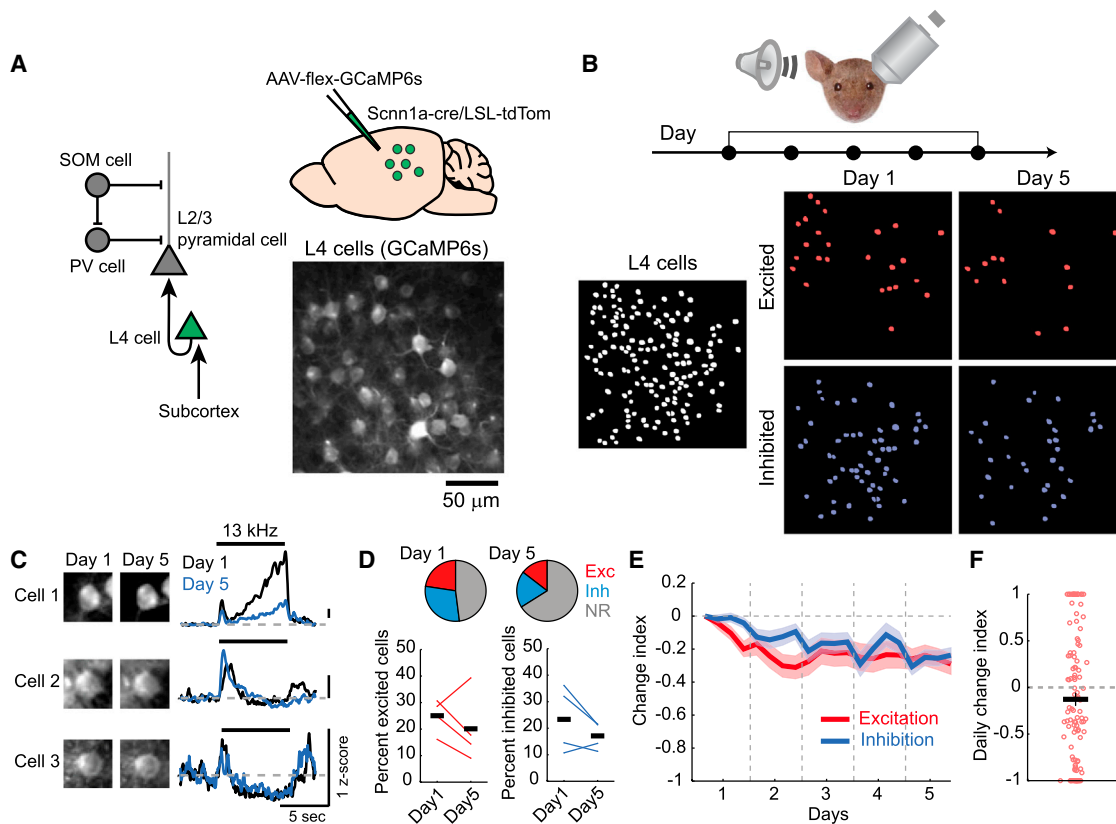


Figure 3. Sound Experience Causes Only a Weak and Balanced Reduction of Excitation and Inhibition in L4 Thalamorecipient Cells

(A) Left: canonical cortical circuit diagram. Top right: GCaMP6s targeting approach. Bottom right: in vivo two-photon image of GCaMP6s-expressing L4 neurons. (B) Top: protocol for sound experience and chronic imaging. Bottom: maps of L4 cell responses in one mouse to 13-kHz tones reveal only a small reduction in the fraction of excited and inhibited cells after daily experience. Bottom left: all imaged cells. (C) Average sound-evoked responses from three L4 cells on day 1 (black) and day 5 (blue). (D) Top: fraction of L4 cells with significant excitatory and inhibitory responses across mice. Bottom: fractions of cells shown separately for individual mice ($n = 4$ mice, 398 cells). (E) Daily experience causes only a small and balanced decrease in the strength of excitatory and inhibitory responses. Average (solid) and SEM (shading) of change index for blocks of 50 trials plotted across days. (F) Daily change index of excitatory responses in individual cells does not show a significant effect of experience from day 1 to day 5 ($n = 99$ excited cells). Error bar represents SEM. See also [Figures S2](#) and [S5](#).

probed the tdTomato-labeled GAD2⁺ cells that were simultaneously imaged in L2/3 during passive experience. However, we found that daily tone experience produced variable effects across this cell population ([Figure S4](#)). We considered the possibility that modest effects at the population level could arise if experience had different and potentially opposing actions on particular subtypes of interneurons. We thus investigated experience-dependent plasticity by separately targeting the two major interneuron subtypes underlying the majority of L2/3 inhibition ([Pfeffer et al., 2013](#)), parvalbumin-expressing and somatostatin-expressing cells, using conditional expression of GCaMP6s in Cre mice (*PV-Cre* and *SOM-IRES-Cre*).

In naive mice, whereas PV cells responded to prolonged pure tones with temporal patterns similar to pyramidal cells, inhibitory responses were more prevalent in the PV cell population ([Figures 4B](#) and [4C](#); excitation: $15.1\% \pm 2.8\%$; inhibition: $46.7\% \pm 2.3\%$; $n = 174$ cells, 5 mice). After 5 days of sound experience, the frac-

tion of PV cells with excitatory responses to the same tones was markedly reduced (day 5: $5.0\% \pm 1.8\%$; day 1 versus day 5, $p = 0.03$), whereas inhibitory responses were significantly enhanced (day 5: $67.1\% \pm 4.5\%$; day 1 versus day 5, $p = 0.01$). In addition, daily experience caused a large reduction in the strength of excitatory responses in PV cells ([Figure 4D](#); $CI = -0.66 \pm 0.07$, $p < 0.001$). Together, these results indicate that the effects of experience on PV cells mirror those of L2/3 pyramidal cells. Importantly, the strong experience-dependent reduction in PV cell activity suggests they are not the source of the enhanced pyramidal cell inhibition during habituation.

Compared to PV cells, prolonged tones evoked distinctly different responses in SOM cells in naive mice: the majority of SOM cells were excited by tones, whereas only a minor fraction of cells were inhibited ([Figures 4E–4G](#); excitation: $69.6\% \pm 6.7\%$; inhibition: $6.4\% \pm 1.1\%$; $n = 112$ cells, 5 mice). Indeed, the ratio between excited and inhibited cells was significantly higher in

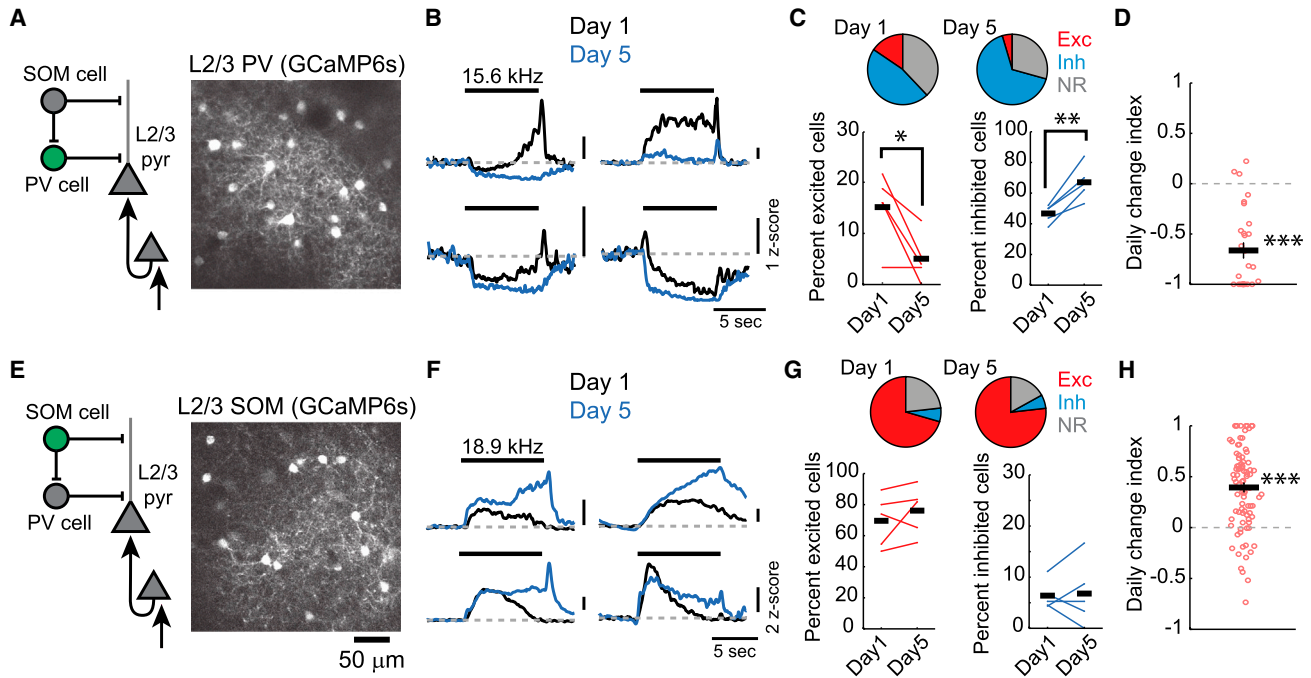


Figure 4. Passive Experience Selectively Enhances Excitatory Responses of SOM Cells

(A) In vivo two-photon image of GCaMP6s-expressing L2/3 PV cells.
 (B) PV cell responses to prolonged tones and the effect of experience mirror pyramidal cells. Average sound-evoked responses from four PV cells on day 1 (black) and day 5 (blue).
 (C) Like pyramidal cells, PV cell excitation becomes sparser and inhibition becomes denser after 5 days of sound experience. Top: fraction of PV cells with significant excitatory and inhibitory responses across mice. Bottom: fraction of cells shown separately for individual mice ($n = 5$ mice, 174 cells).
 (D) Daily change index of excitatory responses in individual PV cells shows a strong reduction in excitation from day 1 to day 5 ($n = 29$ excited cells).
 (E) In vivo two-photon image of GCaMP6s-expressing L2/3 SOM cells.
 (F) Sensory experience increases tone-evoked SOM cell activity. Average sound-evoked responses from four SOM cells on day 1 (black) and day 5 (blue).
 (G) Top: fraction of SOM cells with significant excitatory and inhibitory responses across mice. Bottom: fraction of cells shown separately for individual mice ($n = 5$ mice, 112 cells).
 (H) Daily change index of excitatory responses in individual SOM cells reveals a significant increase in the strength of excitation from day 1 to day 5 ($n = 91$ excited cells).
 Error bars represent SEM. * $p < 0.05$, ** $p < 0.01$, *** $p < 0.001$.
 See also [Figures S2, S4, and S5](#).

SOM cells compared to all other neuron types (SOM cells: 12.5 ± 0.4 ; L2/3 pyramidal cells: 3.0 ± 0.8 ; L4 cells: 1.5 ± 0.5 ; PV cells: 0.34 ± 0.07 ; $p < 0.0001$, one-way ANOVA followed by Tukey's post hoc test). Intriguingly, daily sound experience had a dramatically different action on the responses of SOM cells compared to PV and pyramidal cells: passive tone exposure increased the strength of tone-evoked SOM cell excitation ([Figures 4F and 4H](#); CI = 0.39 ± 0.04 , $p < 0.001$). Indeed, 58.0% of all SOM cells showed significantly larger responses on day 5 compared to day 1, whereas only 9.8% showed the opposite (stronger day 1 responses). Although the fraction of excited cells only slightly increased (day 5: excitation: $76.1\% \pm 6.2\%$; day 1 versus day 5 excitation, $p = 0.32$), this is likely due to the fact that a large majority of SOM cells are already excited by tones before daily experience. Furthermore, the experience-induced enhancement of SOM cell-evoked activity was most prominent during the sustained component of responses, consistent with the pronounced suppression of sustained activity we observed in L2/3 pyramidal cells ([Figure S5](#)). Taken together, these results suggest that the

experience-dependent increase in inhibition of L2/3 pyramidal cells reflects a selective enhancement of sound-evoked activity in SOM-expressing interneurons.

Auditory Cortex Contributes to a Sound Detection Behavioral Task

Our results indicate that repeated daily experience with the same tones induces a habituation of responses in A1 L2/3 through the recruitment of stronger local inhibition. We hypothesized that we might be able to reverse habituation by increasing the behavioral relevance attached to the sound. To test this idea, we investigated whether sensory representations of a habituated tone are enhanced during sound-guided behavior using a sound-offset detection task in head-fixed mice ([Figure 5A](#)). We trained water-restricted mice to lick for a water reward ("hits") during a 1-s time window (answer period) immediately following the offset of the same variable-length (5–9 s) pure tone used for habituation. Trials in which licks occurred during the last 1 s of the tone were terminated and considered "false alarms." Failure

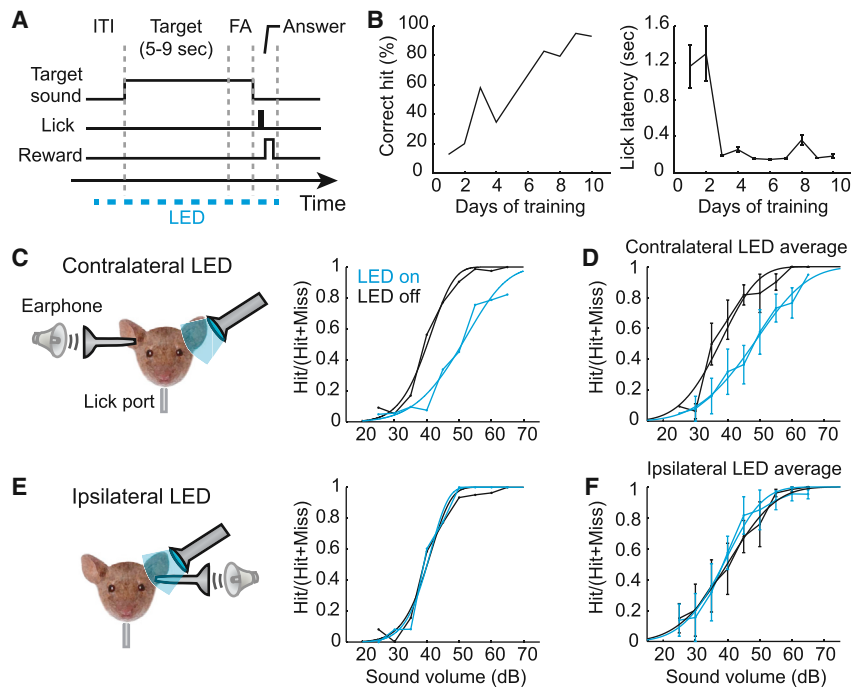


Figure 5. Auditory Cortex Contributes to a Sound-Offset Detection Task

(A) Schematic of the task structure. After the intertrial interval (ITI), a target sound (5- to 9-s pure tone) is delivered. Licking during a 1-s answer period immediately following the target offset triggers a water reward. Licks during the last 1 s of the target sound are false alarms (FAs) and terminate the trial. On randomly interleaved trials, auditory cortex of *VGAT-ChR2* mice is illuminated with LED pulses to silence the cortex. (B) Left: learning curve from a representative mouse. Right: lick latency averaged across trials within each day for the same mouse shown in the left panel. (C) Left: schematic of the experimental setup. Right: representative psychometric curves for behavioral performance during LED_{off} trials (black) and LED_{on} trials (blue) for one mouse. (D) Psychometric curves averaged across all mice (n = 5 mice) with contralateral silencing show a significant increase in detection threshold in LED_{on} trials. (E) Left: schematic of control experiments in the same mice using ipsilateral cortical silencing. Right: psychometric curves for ipsilateral silencing in the same mouse shown in (C). (F) Psychometric curves averaged across all mice with ipsilateral silencing show no change in detection threshold between LED_{on} trials and LED_{off} trials. Error bars represent SEM. See also Figure S6.

to lick during the answer period was scored as a “miss.” Mice learned this behavior rapidly and reached >80% accuracy within 1–2 weeks of daily training (~200 trials/day; Figure 5B). This sound-offset detection configuration gave us the opportunity to monitor sound-evoked activity in A1 without interference from elevated motor function during licking (McGinley et al., 2015; Schneider et al., 2014; Zhou et al., 2014) or reward-triggered activity (Petreanu et al., 2012; Pi et al., 2013).

Whether auditory cortex contributes to the detection of simple sounds in rodents is unclear, because results from previous lesion or pharmacological inactivation studies have ranged from almost no effect to complete deafness (Jaramillo and Zador, 2011; Kelly and Glazier, 1978; Pai et al., 2011; Talwar et al., 2001). Therefore, we first examined whether auditory cortex plays a role in the sound-offset detection task. We tested this by acutely silencing auditory cortex during behavior using transgenic mice (*VGAT-ChR2-EYFP*) that express channelrhodopsin-2 (ChR2) in all GABAergic cells. We implanted a glass window over auditory cortex for LED illumination in these mice and drove GABAergic neurons to suppress activity of excitatory cells (Figure S6). Tones were presented at multiple intensities to measure the psychometric function for sound detection, and contralateral auditory cortex was silenced on 20%–30% of randomly interleaved trials (Figure 5C). Cortical photoinactivation shifted the psychometric curve to the right (n = 5 mice; Figures 5C and 5D), indicating an increase in threshold (63% success rate) for sound detection (LED_{on}: 51.9 ± 4.0 dB; LED_{off}: 40.7 ± 2.6 dB; p = 0.03). In control experiments, LED illumination of ipsilateral cortex in the same mice had no effect on behavior (Figures 5E and 5F), ruling out the possibility of nonspecific effects due to illumination. Curiously, when the contralateral cortical silencing experiments were repeated over several days

the shift of the psychometric curve became progressively smaller, suggesting compensatory changes in subcortical circuits (Figure S6). Taken together, these results show that although subcortical structures alone are sufficient for simple sound detection, auditory cortex plays an important role in improving detection sensitivity.

Sound-Guided Behavior Reverses A1 Habituation

We next tested whether sound representations in A1 change when tones gain behavioral relevance for the animal. Mice expressing GCaMP6s in L2/3 pyramidal cells were trained on the sound-offset detection task after 5 days of habituation to the same tones. Once mice achieved >80% accuracy, we imaged the same populations of A1 cells in alternating blocks of trials (100 trials/block) when mice were performing the task (“behaving”) and when the lick port was removed (“passive”) (Figure 6A). As expected for habituated sensory representations, L2/3 pyramidal cell excitation was sparse and inhibitory responses dominated during the passive block (Figure 6A). Although previous studies have reported changes in A1 sensory representations after learning (Bakin et al., 1996; Blake et al., 2002; Polley et al., 2006; Rutkowski and Weinberger, 2005), we did not observe an increase in sensory representations in the passive condition after training in the simple sound detection task. However, during engagement in the task, the fraction of cells with excitatory responses increased (Figures 6A–6C) (passive: 4.5% ± 2.0%; behaving: 7.5% ± 2.1%; p = 0.04, n = 5 mice, 414 cells) and inhibitory responses were slightly reduced (passive: 45.8% ± 7.9%; behaving: 41.2% ± 9.3%; p = 0.10). Furthermore, a change index comparing the strength of excitatory responses during behaving and passive periods indicated a significant enhancement in excitation during task engagement

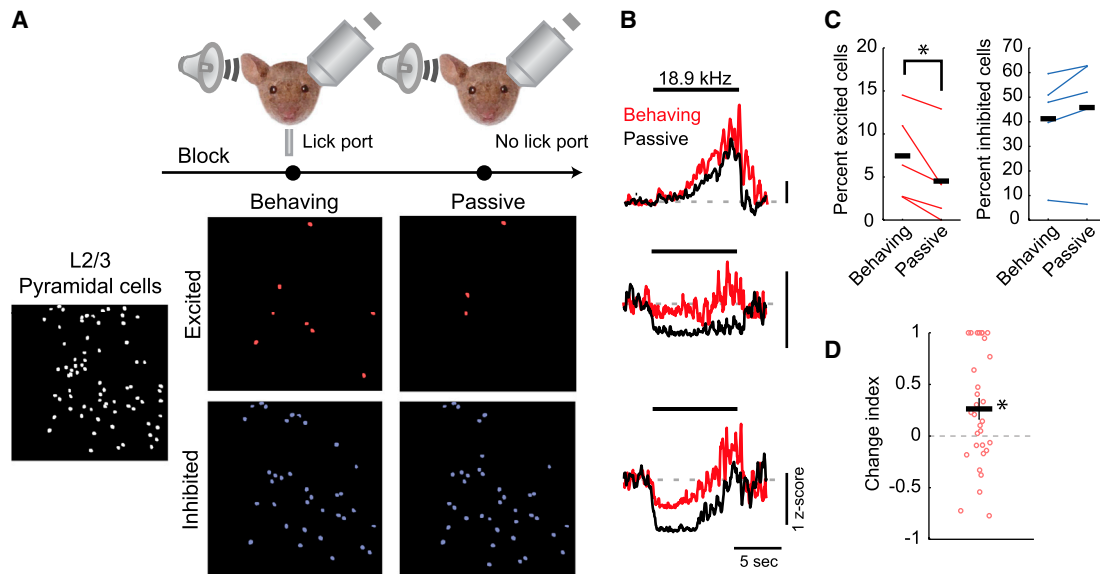


Figure 6. Engagement in Sound-Guided Behavior Enhances L2/3 Sound Representations

(A) Top: schematic showing the protocol for comparing sound representations between behaving and passive blocks within the same day. Bottom: maps of L2/3 pyramidal cell activity during 18.9-kHz tones show that excitation is denser during behavior.

(B) Average sound-evoked responses from three cells during behaving (red) and passive (black) conditions.

(C) Engagement in the behavioral task causes a significant increase in the fraction of cells with excitatory responses ($n = 5$ mice, 414 cells).

(D) Change index indicates an increase in strength of excitatory response during task engagement compared to the passive condition ($n = 31$ excited cells). Error bar represents SEM. $*p < 0.05$.

See also [Figure S7](#).

([Figure 6D](#); $CI = 0.26 \pm 0.10$, $p = 0.01$). As a result, 51.6% of excited cells showed significantly stronger net activity during the behaving block, whereas only 19.4% showed more activity in the passive condition. The effects were not due to the order of passive and behaving blocks ([Figure S7](#)) and were unlikely to result from differences in levels of spontaneous activity, because baseline fluorescence intensity of individual cells was identical during the two conditions (behaving/passive = 0.99 ± 0.04 , $p = 0.85$). These results indicate that sound representations in L2/3 pyramidal cells are enhanced during sound-guided behavior, resulting in the partial reversal of cortical habituation.

We next tested potential sources of the enhanced auditory responses in L2/3 pyramidal cells during behavior. We first studied the impact of sound-guided behavior on sensory representations in mice expressing GCaMP6s in thalamorecipient L4 neurons ([Figure 7A](#)). In contrast to L2/3 pyramidal cells, the fraction of cells responding with tone-evoked excitation or inhibition were identical during passive listening and sound-driven behavior ([Figure 7B](#); excitation passive: $18.4\% \pm 3.6\%$; excitation behaving: $17.5\% \pm 2.0\%$; $p = 0.68$; inhibition passive: $24.2\% \pm 4.9\%$; inhibition behaving: $24.1\% \pm 3.9\%$; $p = 0.98$; $n = 5$ mice, 482 cells). Similarly, the strength of excitatory responses was unchanged between the two conditions ([Figure 7C](#); $CI = -0.02 \pm 0.05$, $p = 0.66$). These results make it unlikely that the enhanced tone-evoked responses in L2/3 pyramidal cells during sound-guided behavior reflect changes in circuits upstream of A1. We repeated the experiments in mice expressing GCaMP6s in SOM and PV cells to explore whether tone-evoked responses of A1 interneurons are modulated by sound-guided

behavior. Intriguingly, sound-guided behavior had the opposite effect on SOM cells compared to L2/3 pyramidal cells ([Figure 7D](#); $n = 4$ mice, 109 cells): the fraction of cells excited by the tone during the behaving block was significantly smaller ([Figure 7E](#)) (passive: $63.0\% \pm 8.1\%$; behaving: $43.8\% \pm 8.6\%$; $p = 0.01$) and the fraction of inhibited cells tended to increase (passive: 7.0 ± 2.4 ; behaving: 16.1 ± 4.5 ; $p = 0.19$). In addition, the strength of tone-evoked excitation across the cell population was markedly reduced during behavior ([Figure 7F](#); $CI = -0.33 \pm 0.04$, $p < 0.001$) and the majority of SOM cells had smaller responses during behaving versus passive blocks (passive response > behaving response: 62.3% ; behaving > passive: 1.4%). Although the very sparse excitation of PV cells following habituation made it difficult to perform a fine comparison, PV cell responses were not obviously different between behaving and passive conditions ([Figures 7G–7I](#)). Taken together, these results suggest that sound-guided behavior acutely enhances sensory representations in A1 via a reduction in local SOM cell-mediated inhibition.

DISCUSSION

In this study, we show that daily passive experience with simple tones causes a marked reduction in the excitatory responses of L2/3 pyramidal cells in primary auditory cortex. This long-lasting form of habituation develops over days and is accompanied by an increase in inhibitory responses to the experienced tones. We find that cortical habituation is unlikely to involve experience-dependent changes relayed to A1 from subcortical regions

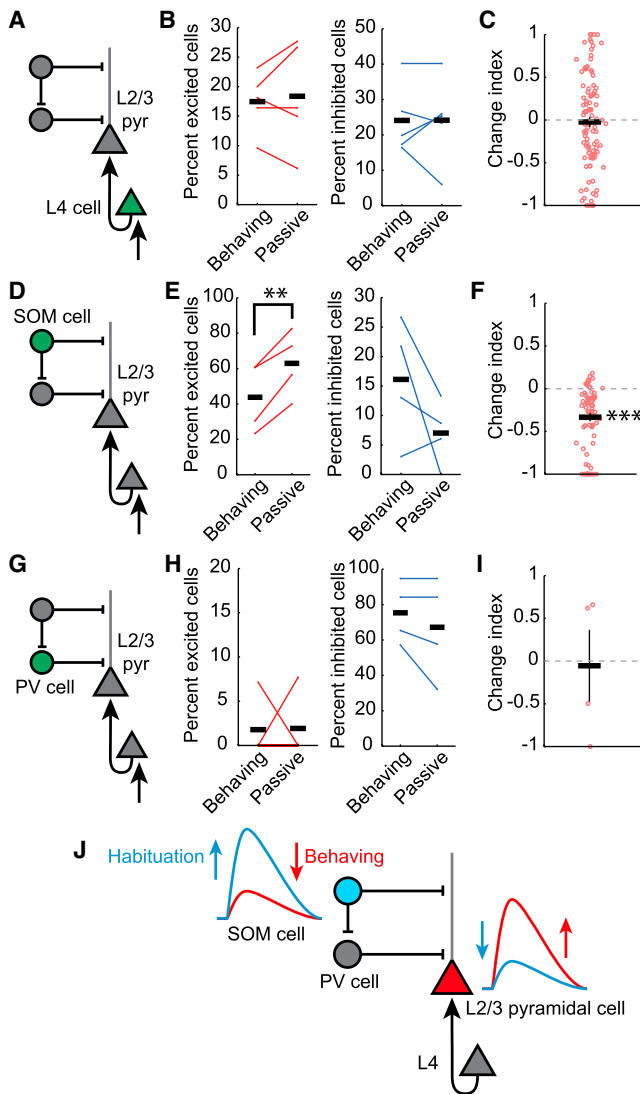


Figure 7. Engagement in Sound-Guided Behavior Suppresses Evoked SOM Cell Activity

(A and B) Imaging L4 excitatory cells reveals no effect of task engagement on the fraction of excited or inhibited cells ($n = 5$ mice, 482 cells). (C) Change index shows no change in excitatory response strength between passive and behaving conditions ($n = 105$ excited cells). (D and E) Imaging L2/3 SOM cells indicates a significant decrease in the fraction of cells with tone-evoked excitation during behavior ($n = 4$ mice, 109 cells). (F) Change index for individual SOM cells shows a marked decrease in the strength of excitatory responses in the behaving versus passive condition ($n = 69$ excited cells). (G and H) Sound-guided behavior has no obvious effect on the fraction of excited or inhibited PV cells ($n = 4$ mice, 92 cells; excitation: $p = 0.97$; inhibition: $p = 0.26$). (I) Change index shows no change in excitatory response strength between passive and behaving conditions ($n = 4$ excited cells, $p = 0.90$). (J) Schematic illustrating the proposed bidirectional modulation of A1 sound representations by SOM cells. Habituation increases SOM cell activity, which leads to decreased sound representations in L2/3 pyramidal cells. In contrast, engagement in sound-guided behavior suppresses SOM cell activity, leading to the enhancement of sound representations in L2/3 pyramidal cells. Error bars represent SEM. ** $p < 0.01$, *** $p < 0.001$.

but rather reflects a selective increase in the activity of local SOM interneurons. We also show that engagement in sound-guided behavior rapidly elicits opposing changes in A1 sound representations; namely, tone-evoked responses of L2/3 pyramidal cells increase, whereas SOM cell excitability is reduced. These results demonstrate that sensory representations in auditory cortex can be flexibly modulated according to the behavioral relevance attached to acoustic stimuli. SOM cells are poised to govern bidirectional changes in A1 sensory representations based on whether stimuli have no significance and should be ignored (habituation) or when the same stimuli become relevant to the animal (sound-guided behavior).

Experience-Dependent Modulation of A1 Sensory Representations

We find that brief daily sound experience in adult mice causes a progressive habituation of L2/3 responses to experienced tones that involves a 10-fold reduction in the excitation/inhibition ratio of population activity. Thus, habituation in A1 is not simply a loss of responsiveness to repeatedly experienced stimuli; rather it reflects an active process that recruits stronger inhibition. Previous studies have implicated inhibitory neurons in cortical plasticity during the critical period (Hensch et al., 1998). Our results are consistent with the idea that GABAergic interneurons also play a role in experience-dependent plasticity later in adulthood. Indeed, sensory experience enhanced the strength of excitatory responses in SOM cells. The fact that PV cells receive strong inhibitory input from SOM cells (Pfeffer et al., 2013) may explain our finding that habituation leads to reduced tone-evoked excitation and increased inhibition of PV cells. These results suggest that habituation in A1 relies on experience-dependent changes in a specific subtype of inhibitory circuit.

Repeated passive exposure to a tone during early critical periods of development results in an overrepresentation of the experienced sound frequency in tonotopic maps of auditory cortex (Barkat et al., 2011; de Villiers-Sidani et al., 2007; Zhang et al., 2001). In contrast, acute recordings from anesthetized animals after long-term sound exposure report that A1 sensory representations are largely refractory to experience-dependent changes in adulthood (Bao et al., 2001; Kilgard and Merzenich, 1998; Zhang et al., 2001; but see Noreña et al., 2006). What accounts for the difference between the lack of effect in previous electrophysiological studies and our results showing strong habituation in L2/3 to experienced stimuli? One possibility reflects differences in the cell populations studied. We found that experience had unique effects on sound representations of L2/3 pyramidal cells, L4 neurons, and SOM cells. Because unit recordings are prone to picking up cells with high firing rates, it is possible that previous experiments have been biased toward recordings of L4 or SOM cells after habituation. Another possibility is the difference in cortical activity between anesthetized and awake animals. For example, the activity of GABAergic interneurons can be strongly attenuated in the anesthetized state (Haider et al., 2013; Kato et al., 2012), and it is possible that inhibition underlying habituation might be more pronounced in the awake state.

Electrophysiological studies in cats have reported perturbed cortical tonotopy after extensive sound exposure (tone bursts

maintained without interruption for 1.5–5 months) (Noreña et al., 2006). However, unlike the results we show, this extensive sound exposure generated a loss of responsiveness at the level of thalamocortical input. Another previous study in cat auditory cortex found that repeated tone exposure could lead to a short-term reduction in responses to experienced tones that recovered within 30 min (Condon and Weinberger, 1991). This does not necessarily conflict with our results, because we also observed modest changes in sound-evoked excitation during the first day of sound experience and habituation progressively accumulated over several days.

We find that the experience-induced enhancement of SOM cell activity was most pronounced during the sustained component of sound-evoked responses. Consistent with this, habituation of L2/3 pyramidal cell activity was more prominent for late responses to prolonged tones compared to responses at sound onset. Sound onsets are likely to signal more critical information (e.g., approach of a predator) than sustained sound features. Thus, the mechanisms we describe may provide animals with the ability to selectively filter out sustained sounds (which are of limited behavioral relevance) while preserving the ability to detect sound onsets. Although we do not exclude the possibility that other mechanisms could contribute to auditory habituation under different conditions, our results suggest that SOM cells can mediate experience-dependent filtering of prolonged sensory input.

Contribution of A1 to Sound Detection

Previous lesion and pharmacological inactivation studies have yielded inconsistent views of the role of auditory cortex in sound detection (Jaramillo and Zador, 2011; Kelly and Glazier, 1978; Pai et al., 2011; Talwar et al., 2001). We took advantage of an acute and reversible optogenetic silencing approach to evaluate the contribution of auditory cortex to a sound-offset detection task. Acute optogenetic silencing of contralateral auditory cortex caused a 10-dB increase in the sound-level threshold for detecting pure tones. Thus, although subcortical systems alone are sufficient for sound detection, auditory cortex contributes to detection sensitivity, most likely via feedback corticofugal projections. This interpretation is consistent with recent work suggesting that A1 amplifies midbrain-dependent sound-evoked escape behavior in mice (Xiong et al., 2015). Interestingly, the 10-dB shift (approximately 3-fold increase in sound pressure) we observe is remarkably similar to the 2- to 3-fold increase in threshold for detection of visual contrast when visual cortex is silenced during a visual detection task (Glickfeld et al., 2013). Sensory cortices governing vision and audition may therefore play similar roles in modulating simple stimulus detection driven by subcortical circuits.

Bidirectional Modulation of A1 Sensory Representations

Although the impact of sound-guided behavior on cortical responses has been explored previously, studies have come to different conclusions. For example, it has been reported that task performance can facilitate evoked responses to auditory stimuli (Fritz et al., 2003; Jaramillo and Zador, 2011), whereas other studies suggest that task engagement only modulates spontaneous cortical activity (Otazu et al., 2009; Rodgers and

DeWeese, 2014). Furthermore, previous studies in auditory cortex have not examined the effects of learning or task engagement in a cell-type-specific manner. Here we show that engagement in sound-guided behavior rapidly reverses the effects of habituation by enhancing sound representations in L2/3 pyramidal cells. This occurs without an increase in L4 activity, indicating that the effects of task engagement are not propagated from subcortical auditory areas. Our results suggest that the suppression of tone-evoked SOM cell activity during sound-guided behavior contributes to the enhanced representation of behaviorally relevant acoustic stimuli. We cannot rule out the possibility that the use of prolonged tones and a sound-offset detection task may account for differences between our findings and previous studies of task engagement that used more transient sound stimuli (Otazu et al., 2009; Rodgers and DeWeese, 2014). Nevertheless, our results reveal a cellular mechanism that contributes to the enhancement of sound representations during active listening to sustained sounds.

Taken together, our results demonstrate the bidirectional modulation of A1 sensory representations by passive experience and engagement in sound-guided behavior and point to SOM cells as a regulator of this flexibility (Figure 7J). What might underlie the regulation of SOM cell activity? One possibility is that SOM cell responses are shaped by neuromodulatory pathways innervating A1 that are differentially engaged in an experience-dependent fashion (Chen et al., 2015; Pinto et al., 2013; Polack et al., 2013). An alternative possibility is that glutamatergic inputs from higher cortical areas directly drive changes in SOM cells. It is also possible that the control of SOM cells from sources extrinsic to auditory cortex utilizes an indirect pathway mediated by other local inhibitory neuron subtypes (Lee et al., 2013; Pfeffer et al., 2013; Pi et al., 2013; Zhou et al., 2014). Although further work is necessary to establish these detailed circuit mechanisms, SOM cells appear to work as a gate in A1 that regulates the flow of auditory information for further processing based on the behavioral relevance of sensory input.

EXPERIMENTAL PROCEDURES

Animals and Surgical Approach

All procedures were in accordance with protocols approved by the UCSD Institutional Animal Care and Use Committee and guidelines of the National Institutes of Health. Mice were acquired from Jackson Laboratories (*Gad2-Cre* [JAX 010802], *PV-Cre* [JAX 008069], *SOM-IRES-Cre* [JAX 013044], *Scnn1a-Cre* [JAX 009613], *VGAT-ChR2-EYFP* [JAX 014548], and *ROSA-LSL-tdTomato* [JAX 007908]) and housed in a room with a reversed light cycle. Experiments were performed during the dark period.

Adult mice (>40 days old, male and female) were anesthetized with isoflurane and injected with dexamethasone (2 mg/kg) intraperitoneally. A custom stainless steel head bar was glued to the skull. Muscle overlying the right auditory cortex was removed and a craniotomy (~2 × 3 mm) was made, leaving the dura intact. Viruses (AAV 2/9-syn-GCaMP6s, AAV 2/9-syn-FLEX-GCaMP6s; Penn Vector Core, University of Pennsylvania) were injected at 5–15 locations (250 μm deep from the pial surface for L2/3 imaging and 400 μm deep for L4 imaging, 20–30 nl/site). A glass window was placed over the craniotomy and secured with dental acrylic. Water restriction (1–2 ml/day) was started 1 week after surgery and mice recovered for an additional 1–2 weeks before imaging. Imaging for habituation and behavior experiments was conducted 28.4 ± 0.9 and 43.8 ± 1.8 days after viral injection, respectively. Pyramidal cells with GCaMP-filled nuclei were excluded from the analyses, because they are reported to show abnormal physiology (Tian et al., 2009). Under our

conditions, only $4.8\% \pm 1.5\%$ (habituation) to $8.1\% \pm 2.4\%$ (behavior) of cells displayed filled nuclei, demonstrating a stable expression in our experiments.

Imaging

Intrinsic signal images were acquired using a tandem lens microscope and 12-bit CCD camera (CCD-1300 QF; VDS Vosskühler). Mice were isoflurane anesthetized and injected with chlorprothixene (0.36 mg/kg, intraperitoneally). Images of surface vasculature were acquired using green LED illumination (540 nm), and intrinsic signals were recorded (27 Hz) using red illumination (615 nm). Each trial consisted of a 1-s baseline followed by a 1-s sound stimulus (75-dB pure tone with a frequency of 3, 10, or 30 kHz, 20 trials for each frequency) and 30-s intertrial interval. Images of reflectance (R) were acquired at $1,024 \times 1,024$ pixels and downsampled to 512×512 pixels by bilinear interpolation. Images during the response period (0.5–2 s from the sound onset) were averaged and divided by the average image during the baseline. Images were averaged across trials and Gaussian filtered. Mice recovered for at least 1 day before two-photon imaging.

GCaMP6s and tdTomato were excited at 920 nm (Mai Tai; Newport), and images (512×512 pixels covering $\sim 500 \times 500 \mu\text{m}$) were acquired with a commercial microscope (B-scope; Thorlabs) running ScanImage software (Vidrio Technologies) using a $16\times$ objective (Nikon) at 28.4 Hz. The fraction of interneurons in L2/3 is estimated to be 26.3% (proportion of GCaMP-expressing cells labeled with tdTomato; $n = 16$ fields from 8 mice). Images were acquired from L2/3 (120–250 μm below the surface) or L4 ($\sim 350 \mu\text{m}$ below the surface). Because our L2/3 imaging was restricted to L2 and superficial L3, it is unlikely that our results were contaminated by thalamorecipient neurons reported in deep L3 (Schiff and Reyes, 2012).

Mouse Behavior

Awake mice were head fixed under the two-photon microscope, and GCaMP6s-expressing cells were imaged in one or two areas within A1. TRFs of individual cells were measured with 1-s pure-tone pips covering 17 frequencies (2–40 kHz, log-spaced) and three volumes (30, 50, and 70 dB SPL). Sound stimuli were presented every 5 s in random order, and each stimulus was presented for five to seven trials. Best frequency for each cell was determined as the frequency that evoked the strongest excitatory response. After constructing the best-frequency map, one area was selected in the middle-frequency (10–20 kHz)-responding region of A1. Stimulus sound frequencies for passive exposure were chosen for individual mice as the frequency that evoked excitation in the largest fraction of cells in the imaged field of view. Mice were exposed to prolonged pure tones (70 dB, tone duration 5, 7, or 9 s, intertrial intervals 9 s) 200 trials/day for 5 days in the head-fixed configuration. Therefore, mice were head fixed for about 1 hr each day, and the total sound exposure was ~ 20 min/day. In both passive exposure and offset-detect behavior experiments (see below), we delivered sounds with three different durations in randomly interleaved trials to avoid the development of temporal expectation (Jaramillo and Zador, 2011). In a subset of animals, TRFs were measured again 1 day after ending the passive exposure protocol.

Behavioral training was started after mice passively experienced the prolonged tones for 5 days as described above. The same sound stimuli used for passive exposure were used for training. Mice were head fixed in front of a lick port and were rewarded with water ($\sim 6 \mu\text{l}/\text{trial}$) for licks during a 1-s answer period immediately following the target sound offset. Licks during the target sound (false alarm) were punished by the elongation of the target sound. Each session lasted ~ 200 trials (1–2 hr). In the optogenetic experiments, the false-alarm period was set as the last 1 s of the target sound, and licks during this period terminated the trial. To correct for the overestimation of hit rates caused by false-alarm responses, we removed correct trials that can be accounted for by the false-alarm rate (Glickfeld et al., 2013). In imaging experiments, the false-alarm period was the entire duration of the sound, so that sound-evoked cellular activity occurred in the absence of licking. After mice performed 100 trials of offset-detect behavior (behaving block), the lick port was removed and mice quickly stopped attempting to lick. Mice were passively exposed to the same sound stimuli for 100 trials (passive block). In a subset of experiments, the lick port was placed in front of the mouse again, and mice performed an additional 100 trials of offset-detect behavior. Licks were detected by breaking an infrared beam (Island Motion), and water deliv-

ery was controlled by a solenoid valve (NResearch). The behavioral setup was controlled by software (Dispatcher; <http://brodylab.org>) running on MATLAB (MathWorks) communicating with a real-time system (RTLinux).

Auditory stimuli were delivered via a free-field electrostatic speaker (ES1; Tucker-Davis Technologies). In experiments described in Figure 5 and Figure S6C, a coupler model electrostatic speaker (ES1) was connected to a custom-made stainless steel earphone directly inserted into the ear canal. Speakers were calibrated over a range of 2–40 kHz to give a flat response (± 1 dB). Stimuli were delivered to the ear contralateral to the chronic window, unless otherwise noted.

Image Analysis

Lateral motion was corrected by cross-correlation-based image alignment. Regions of interest (ROIs) corresponding to visually identifiable cells were manually drawn, and pixels within each ROI were averaged to create a fluorescence time series, $F_{\text{cell_measured}}(t)$. To correct for neuropil contamination (Chen et al., 2013), ring-shaped background ROIs (starting at 2 pixels and ending at 8 pixels from the border of the ROI) were created around each cell ROI. From this background ROI, pixels that contained cell bodies or processes from surrounding cells were excluded. The remaining pixels were averaged to create a background fluorescence time series, $F_{\text{background}}(t)$. The correlation coefficient between $F_{\text{cell_measured}}(t)$ and $F_{\text{background}}(t)$ measured 0.552 ± 0.004 . The fluorescence signal of a cell body was estimated as $F_{\text{cell_true}}(t) = F_{\text{cell_measured}}(t) - 0.9 \times F_{\text{background}}(t)$. To ensure robust neuropil subtraction, only cell ROIs that were at least 3% brighter than the background ROIs were included. Although we cannot exclude some residual contamination of cellular signals by neuropil responses, our conclusions are not dependent on the degree of background subtraction (Figure S2). To account for slow drifts in absolute fluorescence intensity, a normalized trace, $F_{\text{norm}}(t)$, was calculated as $F_{\text{cell_true}}(t)/F_0(t)$, where $F_0(t)$ is a time-varying drifting trace estimated by smoothing inactive portions of $F_{\text{cell_true}}(t)$ using an iterative procedure. $F_{\text{norm}}(t)$ was LOESS smoothed with a 1-s window and subsequently used for spike probability inference based on a fast, nonnegative deconvolution method (Vogelstein et al., 2010). Inferred spikes were then sorted into separate traces for individual trials, $S_{\text{trial}}(t)$, based on the time of sound delivery. Z score was calculated as $(S_{\text{trial}}(t) - \mu)/\sigma$, where μ refers to the mean during baseline in individual trials (2.5-s period preceding sound onset) and σ refers to the SD calculated from concatenating traces of the baselines from all trials within each day. This Z score trace was used for subsequent statistical analyses.

Cells were judged as significantly excited (inhibited) if they fulfilled two criteria: (1) the area above baseline for individual trials was significantly larger (smaller) than zero using the Wilcoxon signed-rank test, and (2) the peak positive-going (negative-going) amplitude exceeded a fixed threshold value. Because tone durations varied between 5, 7, and 9 s, statistical analyses were performed on the first 5 s of tones. Threshold for excitation (1.0 Z score) was determined by receiver operator characteristic (ROC) analysis to yield a 90% true positive rate in TRF measurements. Because inhibitory responses tend to be small in amplitude (Boyd et al., 2015; Peron et al., 2015), the threshold for inhibition was set as half that for excitation (-0.5 Z score) to increase detection sensitivity. Raising the threshold to -1.0 Z score reduced the number of detected responses but did not qualitatively affect our findings. The average sound-evoked response trace for each cell was derived from a composite of responses to the three tone durations across trials. Area above baseline of the average trace during tones was used for the calculation of change index as $\text{CI} = (\text{area}_{\text{after}} - \text{area}_{\text{before}})/(\text{area}_{\text{after}} + \text{area}_{\text{before}})$. CIs were calculated separately for excitatory and inhibitory responses, and only cells judged as responsive were included in the analysis. For the CI time course plots, areas were calculated for individual 50-trial blocks on each day, and they were compared to the area on the initial block of day 1. Daily CI between day 5 and day 1 was calculated using the second half of trials on each day to ensure that daily responses stabilized after the onset of imaging. Unless otherwise stated, all statistical comparisons were performed using a two-tailed t test.

Unit Recording and Cortical Silencing

On the day before recording, adult *VGAT-ChR2* mice were anesthetized with isoflurane and injected with dexamethasone (2 mg/kg). A head bar was

implanted, and the skull over auditory cortex was thinned and covered with cyanoacrylate glue. A1 was identified by intrinsic signal imaging, and a craniotomy (<500- μ m diameter) was made over the middle-frequency area. The craniotomy was covered with silicone elastomer between recordings. On the day of recording, a 16-channel silicon probe (NeuroNexus; A1x16-5mm-50 s-177-A16) was inserted into A1 of awake, head-fixed mice. Unit activity was amplified (A-M Systems), digitized (National Instruments), and acquired at 20 kHz with custom software in MATLAB. Prolonged pure tones (60 or 70 dB, 18.9 kHz, duration 9 s, intertrial interval 17 s) were delivered to the ear contralateral to the recording. Units were isolated using an open-source, K-means clustering algorithm and spike-sorting graphical user interface (UltraMegasort2000; <https://physics.ucsd.edu/neurophysics>).

For cortical silencing during behavior, a glass window was implanted over the right auditory cortex of *VGAT-ChR2* mice as described above. After training in the tone-offset detection task, a fiber-coupled LED (~20 mW, 470 nm, 1-mm fiber, 0.48 N.A.; Doric Lenses) was positioned 1–2 mm above the glass window. In 30% of randomly interleaved trials, we delivered a train of light pulses (10 ms, 20 Hz) to silence auditory cortex. Light pulses lasted from 2 s before sound onset to 1 s after sound offset. Licks during the false-alarm or answer period terminated the LED. In unit recording experiments to confirm cortical silencing, the LED was positioned above the thinned skull. The LED was turned on 2 s after the sound onset and lasted for 2 s on 50% of the trials.

SUPPLEMENTAL INFORMATION

Supplemental Information includes seven figures and can be found with this article online at <http://dx.doi.org/10.1016/j.neuron.2015.10.024>.

ACKNOWLEDGMENTS

We thank M. Scanziani for helpful discussions and L.L. Looger, J. Akerboom, D.S. Kim, and the GENIE Project at Janelia Farm Research Campus for making GCaMP available. We are grateful to A. Mitani, A.J. Peters, and T. Komiyama for sharing analysis code. H.K.K. is a JSPS Postdoctoral Fellow for Research Abroad. Supported by NIH R01DC04682 (to J.S.I.).

Received: July 18, 2015

Revised: September 10, 2015

Accepted: October 13, 2015

Published: November 12, 2015

REFERENCES

- Anderson, L.A., Christianson, G.B., and Linden, J.F. (2009). Stimulus-specific adaptation occurs in the auditory thalamus. *J. Neurosci.* 29, 7359–7363.
- Bakin, J.S., and Weinberger, N.M. (1996). Induction of a physiological memory in the cerebral cortex by stimulation of the nucleus basalis. *Proc. Natl. Acad. Sci. USA* 93, 11219–11224.
- Bakin, J.S., South, D.A., and Weinberger, N.M. (1996). Induction of receptive field plasticity in the auditory cortex of the guinea pig during instrumental avoidance conditioning. *Behav. Neurosci.* 110, 905–913.
- Bandyopadhyay, S., Shamma, S.A., and Kanold, P.O. (2010). Dichotomy of functional organization in the mouse auditory cortex. *Nat. Neurosci.* 13, 361–368.
- Bao, S., Chan, V.T., and Merzenich, M.M. (2001). Cortical remodelling induced by activity of ventral tegmental dopamine neurons. *Nature* 412, 79–83.
- Barkat, T.R., Polley, D.B., and Hensch, T.K. (2011). A critical period for auditory thalamocortical connectivity. *Nat. Neurosci.* 14, 1189–1194.
- Blake, D.T., Strata, F., Churchland, A.K., and Merzenich, M.M. (2002). Neural correlates of instrumental learning in primary auditory cortex. *Proc. Natl. Acad. Sci. USA* 99, 10114–10119.
- Boyd, A.M., Kato, H.K., Komiyama, T., and Isaacson, J.S. (2015). Broadcasting of cortical activity to the olfactory bulb. *Cell Rep.* 10, 1032–1039.
- Chen, T.-W., Wardill, T.J., Sun, Y., Pulver, S.R., Renninger, S.L., Baohan, A., Schreiter, E.R., Kerr, R.A., Orger, M.B., Jayaraman, V., et al. (2013). Ultrasensitive fluorescent proteins for imaging neuronal activity. *Nature* 499, 295–300.
- Chen, N., Sugihara, H., and Sur, M. (2015). An acetylcholine-activated micro-circuit drives temporal dynamics of cortical activity. *Nat. Neurosci.* 18, 892–902.
- Condon, C.D., and Weinberger, N.M. (1991). Habituation produces frequency-specific plasticity of receptive fields in the auditory cortex. *Behav. Neurosci.* 105, 416–430.
- Desimone, R., and Duncan, J. (1995). Neural mechanisms of selective visual attention. *Annu. Rev. Neurosci.* 18, 193–222.
- de Villers-Sidani, E., Chang, E.F., Bao, S., and Merzenich, M.M. (2007). Critical period window for spectral tuning defined in the primary auditory cortex (A1) in the rat. *J. Neurosci.* 27, 180–189.
- DeWeese, M.R., Wehr, M., and Zador, A.M. (2003). Binary spiking in auditory cortex. *J. Neurosci.* 23, 7940–7949.
- Fritz, J., Shamma, S., Elhilali, M., and Klein, D. (2003). Rapid task-related plasticity of spectrotemporal receptive fields in primary auditory cortex. *Nat. Neurosci.* 6, 1216–1223.
- Froemke, R.C., Carcea, I., Barker, A.J., Yuan, K., Seybold, B.A., Martins, A.R.O., Zaika, N., Bernstein, H., Wachs, M., Levis, P.A., et al. (2013). Long-term modification of cortical synapses improves sensory perception. *Nat. Neurosci.* 16, 79–88.
- Glickfeld, L.L., Histed, M.H., and Maunsell, J.H.R. (2013). Mouse primary visual cortex is used to detect both orientation and contrast changes. *J. Neurosci.* 33, 19416–19422.
- Guo, W., Chambers, A.R., Darrow, K.N., Hancock, K.E., Shinn-Cunningham, B.G., and Polley, D.B. (2012). Robustness of cortical topography across fields, laminae, anesthetic states, and neurophysiological signal types. *J. Neurosci.* 32, 9159–9172.
- Haider, B., Häusser, M., and Carandini, M. (2013). Inhibition dominates sensory responses in the awake cortex. *Nature* 493, 97–100.
- Hensch, T.K., Fagiolini, M., Mataga, N., Stryker, M.P., Baekkeskov, S., and Kash, S.F. (1998). Local GABA circuit control of experience-dependent plasticity in developing visual cortex. *Science* 282, 1504–1508.
- Issa, J.B., Haeffele, B.D., Agarwal, A., Bergles, D.E., Young, E.D., and Yue, D.T. (2014). Multiscale optical Ca²⁺ imaging of tonal organization in mouse auditory cortex. *Neuron* 83, 944–959.
- Jaramillo, S., and Zador, A.M. (2011). The auditory cortex mediates the perceptual effects of acoustic temporal expectation. *Nat. Neurosci.* 14, 246–251.
- Kato, H.K., Chu, M.W., Isaacson, J.S., and Komiyama, T. (2012). Dynamic sensory representations in the olfactory bulb: modulation by wakefulness and experience. *Neuron* 76, 962–975.
- Kelly, J.B., and Glazier, S.J. (1978). Auditory cortex lesions and discrimination of spatial location by the rat. *Brain Res.* 145, 315–321.
- Kilgard, M.P., and Merzenich, M.M. (1998). Cortical map reorganization enabled by nucleus basalis activity. *Science* 279, 1714–1718.
- Lee, S., Kruglikov, I., Huang, Z.J., Fishell, G., and Rudy, B. (2013). A disinhibitory circuit mediates motor integration in the somatosensory cortex. *Nat. Neurosci.* 16, 1662–1670.
- Luczak, A., Bartho, P., and Harris, K.D. (2013). Gating of sensory input by spontaneous cortical activity. *J. Neurosci.* 33, 1684–1695.
- Lütcke, H., Gerhard, F., Zenke, F., Gerstner, W., and Helmchen, F. (2013). Inference of neuronal network spike dynamics and topology from calcium imaging data. *Front. Neural Circuits* 7, 201.
- Malmierca, M.S., Cristaudo, S., Pérez-González, D., and Covey, E. (2009). Stimulus-specific adaptation in the inferior colliculus of the anesthetized rat. *J. Neurosci.* 29, 5483–5493.

- McGinley, M.J., David, S.V., and McCormick, D.A. (2015). Cortical membrane potential signature of optimal states for sensory signal detection. *Neuron* 87, 179–192.
- Niell, C.M., and Stryker, M.P. (2010). Modulation of visual responses by behavioral state in mouse visual cortex. *Neuron* 65, 472–479.
- Noreña, A.J., Gourévitch, B., Aizawa, N., and Eggmونت, J.J. (2006). Spectrally enhanced acoustic environment disrupts frequency representation in cat auditory cortex. *Nat. Neurosci.* 9, 932–939.
- Otazu, G.H., Tai, L.-H., Yang, Y., and Zador, A.M. (2009). Engaging in an auditory task suppresses responses in auditory cortex. *Nat. Neurosci.* 12, 646–654.
- Pai, S., Erlich, J.C., Kopec, C., and Brody, C.D. (2011). Minimal impairment in a rat model of duration discrimination following excitotoxic lesions of primary auditory and prefrontal cortices. *Front. Syst. Neurosci.* 5, 74.
- Peron, S.P., Freeman, J., Iyer, V., Guo, C., and Svoboda, K. (2015). A cellular resolution map of barrel cortex activity during tactile behavior. *Neuron* 86, 783–799.
- Petreaanu, L., Gutnisky, D.A., Huber, D., Xu, N.L., O'Connor, D.H., Tian, L., Looger, L., and Svoboda, K. (2012). Activity in motor-sensory projections reveals distributed coding in somatosensation. *Nature* 489, 299–303.
- Pfeffer, C.K., Xue, M., He, M., Huang, Z.J., and Scanziani, M. (2013). Inhibition of inhibition in visual cortex: the logic of connections between molecularly distinct interneurons. *Nat. Neurosci.* 16, 1068–1076.
- Pi, H.-J., Hangya, B., Kvitsiani, D., Sanders, J.I., Huang, Z.J., and Kepecs, A. (2013). Cortical interneurons that specialize in disinhibitory control. *Nature* 503, 521–524.
- Pinto, L., Goard, M.J., Estandian, D., Xu, M., Kwan, A.C., Lee, S.-H., Harrison, T.C., Feng, G., and Dan, Y. (2013). Fast modulation of visual perception by basal forebrain cholinergic neurons. *Nat. Neurosci.* 16, 1857–1863.
- Polack, P.-O., Friedman, J., and Golshani, P. (2013). Cellular mechanisms of brain state-dependent gain modulation in visual cortex. *Nat. Neurosci.* 16, 1331–1339.
- Polley, D.B., Steinberg, E.E., and Merzenich, M.M. (2006). Perceptual learning directs auditory cortical map reorganization through top-down influences. *J. Neurosci.* 26, 4970–4982.
- Rodgers, C.C., and DeWeese, M.R. (2014). Neural correlates of task switching in prefrontal cortex and primary auditory cortex in a novel stimulus selection task for rodents. *Neuron* 82, 1157–1170.
- Rothschild, G., Nelken, I., and Mizrahi, A. (2010). Functional organization and population dynamics in the mouse primary auditory cortex. *Nat. Neurosci.* 13, 353–360.
- Rutkowski, R.G., and Weinberger, N.M. (2005). Encoding of learned importance of sound by magnitude of representational area in primary auditory cortex. *Proc. Natl. Acad. Sci. USA* 102, 13664–13669.
- Schiff, M.L., and Reyes, A.D. (2012). Characterization of thalamocortical responses of regular-spiking and fast-spiking neurons of the mouse auditory cortex in vitro and in silico. *J. Neurophysiol.* 107, 1476–1488.
- Schneider, D.M., Nelson, A., and Mooney, R. (2014). A synaptic and circuit basis for corollary discharge in the auditory cortex. *Nature* 513, 189–194.
- Schreiner, C.E., Froemke, R.C., and Atencio, C. (2010). Spectral processing in auditory cortex. In *The Auditory Cortex*, J.A. Winer and C.E. Schreiner, eds. (Springer), pp. 275–308.
- Sutter, M.L. (2000). Shapes and level tolerances of frequency tuning curves in primary auditory cortex: quantitative measures and population codes. *J. Neurophysiol.* 84, 1012–1025.
- Talwar, S.K., Musial, P.G., and Gerstein, G.L. (2001). Role of mammalian auditory cortex in the perception of elementary sound properties. *J. Neurophysiol.* 85, 2350–2358.
- Tian, L., Hires, S.A., Mao, T., Huber, D., Chiappe, M.E., Chalasani, S.H., Petreaanu, L., Akerboom, J., McKinney, S.A., Schreiter, E.R., et al. (2009). Imaging neural activity in worms, flies and mice with improved GCaMP calcium indicators. *Nat. Methods* 6, 875–881.
- Ulanovsky, N., Las, L., and Nelken, I. (2003). Processing of low-probability sounds by cortical neurons. *Nat. Neurosci.* 6, 391–398.
- Vogelstein, J.T., Packer, A.M., Machado, T.A., Sippy, T., Babadi, B., Yuste, R., and Paninski, L. (2010). Fast nonnegative deconvolution for spike train inference from population calcium imaging. *J. Neurophysiol.* 104, 3691–3704.
- Volkov, I.O., and Galazjuk, A.V. (1991). Formation of spike response to sound tones in cat auditory cortex neurons: interaction of excitatory and inhibitory effects. *Neuroscience* 43, 307–321.
- Wang, X., Lu, T., Snider, R.K., and Liang, L. (2005). Sustained firing in auditory cortex evoked by preferred stimuli. *Nature* 435, 341–346.
- Xiong, X.R., Liang, F., Zingg, B., Ji, X.-Y., Ibrahim, L.A., Tao, H.W., and Zhang, L.I. (2015). Auditory cortex controls sound-driven innate defense behaviour through corticofugal projections to inferior colliculus. *Nat. Commun.* 6, 7224.
- Zhang, L.I., Bao, S., and Merzenich, M.M. (2001). Persistent and specific influences of early acoustic environments on primary auditory cortex. *Nat. Neurosci.* 4, 1123–1130.
- Zhou, M., Liang, F., Xiong, X.R., Li, L., Li, H., Xiao, Z., Tao, H.W., and Zhang, L.I. (2014). Scaling down of balanced excitation and inhibition by active behavioral states in auditory cortex. *Nat. Neurosci.* 17, 841–850.